 DOI: 10.1002/masy.200900007

In Line Spectroscopic Investigation of Fluorinated Copolymer Synthesis in Supercritical Carbon Dioxide

*Eléonore Möller, Ulrike Schreiber, Sabine Beuermann**

Summary: In-line Fourier Transform – near infrared (FT-NIR) spectroscopy is a very elegant method to follow conversion as well as phase behaviour throughout a reaction. It was applied to two examples of homogeneous phase syntheses of fluorinated copolymers in supercritical carbon dioxide ($scCO_2$). The conventional free radical copolymerization of vinylidene fluoride (VDF) and hexafluoropropene (HFP) on the one hand side, and the Activators Generated by Electron Transfer (AGET) Atom Transfer Radical Polymerization (ATRP) of F-decene (1H-1H, 2H perfluoro-1-decene) and *t*BA (*tert*-butyl acrylate) on the other hand side were studied. Poly(VDF-co-HFP) were synthesized at 75 and 100 °C at pressures above 800 bar to remain in solution, even at high VDF contents. The reactivity ratios, *r*, were determined from a small number of experiments using the entire conversion vs. time data from in-line FT-NIR measurements. The estimated values are $r_{VDF} = 4.3$ and $r_{HFP} = 0.1$. In the case of poly(F-decene-co-*t*BA), a fluorinated macroligand was introduced for AGET ATRP. Molecular weights between 10000 and 40000 g/mol and polydispersities between 1.1 and 2.1 were obtained while remaining in homogeneous phase. Reactivity ratios were determined as $r_{F\text{-}decene} = 0.02$ and $r_{tBA} = 9.1$.

Keywords: AGET ATRP; copolymerization; fluoropolymers; FT-IR; supercritical CO_2

Introduction

In-line monitoring of copolymerizations, in particular via in-line FT-NIR spectroscopy, is a powerful tool that offers detailed insights into the mechanisms and phase behavior of such reactions. The ability to follow the real-time conversion of individual monomers acting in the copolymerization is of major importance for quantitative investigation of the kinetics involved. The macroscopic phase behavior can also be qualitatively observed due to the simple fact that as soon as the reaction system becomes heterogeneous, the incident NIR light is increasingly scattered, which will result in a baseline shift towards higher absorbances of the spectra.[1]

In-line FT-NIR spectroscopy may be used to determine monomer feed ratio and copolymer composition over the full conversion range, contrary to the classical approach that necessitates numerous independent experiments up to small conversion for scanning a wide range of monomer feed ratios. Reducing the number of experiments is of particular interest in the case of high pressure copolymerizations that are rather laborious, and are also limited with respect to reaction volumes (and therefore amount of product available for analysis etc...) due to safety reasons.

Polymerizations in supercritical carbon dioxide ($scCO_2$) gained a lot of interest in the past decades.[2] Besides being environmentally benign, interesting features of $scCO_2$ for polymer applications are a reduction in viscosity, easy separation from polymeric products under mild conditions and particle generation upon expansion of the reaction mixture. Although the solubility of most polymers in $scCO_2$ is limited, the presence of fluorocarbon pendent groups on a hydrocarbon backbone showed

Institute of Chemistry, University of Potsdam, Karl-Liebknecht Str. 24-25, D 14476 Golm / Potsdam, Germany
E-mail: sabine.beuermann@uni-potsdam.de

to be advantageous for the homogeneity of fluoropolymer/scCO$_2$ systems.[3] Fluorinated polymers are usually synthesized in heterogeneous phase (in water or organic solvents) and require the use of fluorinated stabilizers, which have a high potential for bioaccumulation.[4] ScCO$_2$ has naturally emerged as an attractive alternative reaction medium for the synthesis of these polymers in solution, in which the above mentioned stabilizers are no longer required.[5,6] Alternately, precipitation polymerizations are feasible, which, however, are often associated with a high polydispersity of the molecular weight distribution.[7–10]

The efforts to produce fluorinated polymers under supercritical conditions are compensated by the fact that they are high value polymers employed for technical applications. They possess unique properties, e.g., excellent chemical, thermal, and mechanical stability.[11,12] For instance, copolymers of fluoroalkenes and acrylates provide good adhesion forces with non-polar surfaces and low surface tensions.[13] Vinylidene fluoride (VDF) homo- and copolymers are of particular interest due to their ferroelectricity[14,15] leading to applications, e.g., in transducers, sensors or switches. In the case of vinylidene fluoride – hexafluoropropene copolymers, the properties are also influenced by the hexafluoropropene (HFP) content in the copolymer, since this parameter controls the crystallinity of the material.

Controlled radical polymerization methods are known to give access to well defined copolymer architectures, e.g. block, graft, star copolymers, and materials with well controlled molecular weights. While in the past these techniques were mostly applied to non-fluorinated polymerization, we used the so-called AGET ATRP method (Activators Generated by Electron Transfer Atom Transfer Radical Polymerization)[16] for copolymerizations of 1H,1H,2H-perfluoro-1-decene (F-decene) and *tert*-butyl acrylate (*t*BA). AGET ATRP allows for controlled radical polymerizations with very low amounts of copper, since the active Cu^I species is retained from the Cu^{II} by a reducing agent. For mechanistic details the reader is referred to the original work by the group of Matyjaszewski.[16]

Herein we report homogeneous phase free radical copolymerizations of VDF and HFP as well as AGET ATRP of F-decene and *tert*-butyl acrylate in solution with scCO$_2$. To allow for homogeneous reaction mixtures rather high pressures in the kbar range were applied. Moreover, controlled radical polymerizations were reported to benefit from high pressures.[17,18] Copolymerization reactivity ratios were calculated from a rather small number of high-pressure experiments with in-line conversion measurements and non-linear regression analyses.

Experimental

Materials

The monomers vinylidene fluoride (VDF, 99% provided by Dyneon GmbH) and hexafluoropropene (HFP, 99% provided by Dyneon GmbH), the initiators di-*tert* butyl peroxide (DTBP, 99% Trigonox B, AKZO Nobel) and *tert*-butyl peroxypivalate (TBPP, 75% solution, Trigonox 25 C75, AKZO Nobel) for reactions at 100 and 75 °C, respectively, carbon dioxide (CO$_2$, grade 4.5, Air Liquide), the eluent for size-exclusion chromatography hexafluoroisopropanol (HFIP, Fluorochem, 99%) containing potassium trifluoroacetate (> 99% p.a., Fluka) were used as received.

Tert-butyl acrylate (*t*BA) (Alfa Aesar, 99%) were passed through a column with inhibitor remover (Aldrich) and stored under inert gas atmosphere at 7 °C. 1H, 1H, 2H perfluoro-1-decene (F-decene, Alfa Aesar, 99%), 1-octene (Aldrich, 98%), CuBr$_2$ (Acros, 99%), tin (II)-2 ethylhexanoate (Sn(EH)$_2$, Aldrich, 95%) and the initiators ethyl α-bromoisobutyrate (EBIB, Merck, 98%) as well as *tert*-butyl peroxy-2-ethylhexanoate (TBPO, Akzo Nobel, 99.2%) were used as received. The fluorinated ligand F-TEDETA given in Scheme 1 was synthesized as reported elsewhere.[19]

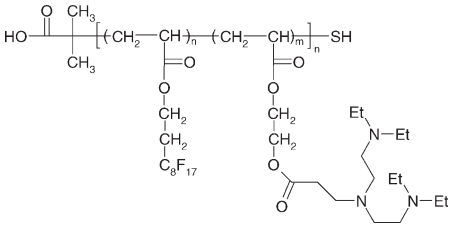

Scheme 1.
Structure of the fluorinated ligand F-TEDETA used for AGET ATRP in $scCO_2$.

Measurement of VDF and HFP Reference Spectra

Gaseous monomers were condensed into 23 mL auxiliary autoclaves cooled to approximately $-10\,^{\circ}C$ with a maximum pressure of 300 bar. These autoclaves are suitable for pressures up to 500 bar and equipped with a rupture disc set to 500 bar.[20] The filled autoclave was allowed to warm up until condensed water on the walls could be wiped out, and then was weighted using a Kern PCB 1600-2 balance. For measurements of HFP spectra the high pressure cell was evacuated and in the case of VDF about 0.2 mL of α-pinene serving as inhibitor was introduced. The small amount of α-pinene does not interfere with the NIR absorption bands of VDF. After transferring monomer from the small autoclave to the high pressure cell, the autoclaves were weighted again. The mass of monomer injected into the cell of known volume was determined with a precision of ± 0.1 g.

Reference spectra of the pure monomers were taken at room temperature and reaction temperature. Then, CO_2 was added to reach the reaction pressures and check the influence of pressure on the spectra. HFP spectra in the mid-infrared range and VDF spectra in the near-infrared range were measured with silicon and sapphire windows, respectively.

Apparatus and Procedure for Conventional FRP of VDF and HFP in $scCO_2$

The reaction mixtures were prepared using the set-up detailed in ref.[6]. The initiator was filled into the inlet for liquid components and by passing CO_2 through the initiator O_2 dissolved in the initiator was removed. Then, the initiator was transferred into the mixing autoclave. The monomer HFP was compressed and pumped by the pneumatically driven pump. The volume of HFP added to the mixing autoclave was controlled by the syringe pump. A first portion (volume controlled by syringe pump) of CO_2 was compressed and pumped by a second pneumatically driven pump and filled into the mixing autoclave, ensuring that residual HFP is transferred into the mixing autoclave. The same procedure was applied to add VDF into the mixing autoclave. Again the remaining portion of CO_2 was compressed, pumped and added to the autoclave. The mixture consisting of initiator, CO_2, HFP and VDF inside the mixing autoclave was stirred with a magnetic stir bar for one hour at a pressure of 350 bar to ensure homogeneous mixing of the components. To prevent polymerization, the mixing autoclave was cooled to $0\,^{\circ}C$. This method of mixture preparation allows for monomer concentrations with a precision of $\pm\ 0.1\,mol \cdot L^{-1}$ if their densities are accurately known.

Then, the mixture was transferred to the syringe pump and the pre-heated optical high-pressure cell equipped with two sapphire windows, which is directly placed in the sample compartment of the FT-NIR spectrometer. To avoid demixing during the filling procedure an HPLC pump was employed to keep the pressure constant by moving the piston of the mixing autoclave, and thus, reducing the volume. The final pressure inside the optical cell - measured using a pressure gauge from HBM (P3MB) - was adjusted with the syringe pump. A detailed description of the set-up and of the preparation method of VDF rich mixtures was previously reported.[6]

Volume contraction occurs throughout the polymerization since the density of the polymer produced is higher than that of the gaseous monomers and the volume of the above mentioned cell is constant. Therefore the initial pressure (p_0) is higher than the final pressure (p_f).

Procedure for AGET ATRP in $scCO_2$

$CuBr_2$, ligand and reducing agent were filled in a 10 mL round bottom flask and bubbled with nitrogen before the oxygen-free monomers are added via a degassed syringe. The high pressure cell equipped with a Teflon coated magnetic stirring bar is filled with this mixture and closed under inert gas atmosphere. Then, the cell is filled with CO_2 up to a pressure of 400 bar and heated to polymerization temperature. The final pressure was 1000 bar.

Characterization

Size exclusion chromatography (SEC) of poly(*t*BA-co-F-decene) was carried out with hexafluoroisopropanol containing potassium trifluoroacetate (0.05 *M*) as eluent and a column temperature of 23 °C. The samples were analyzed on a SEC set-up consisting of an Agilent 1200 isocratic pump, an Agilent 1200 refractive index detector with PSS-WinGPC software, and two PFG columns (7 μm, 8 × 300 mm, pore sizes 100 and 300 Å) from PSS. The SEC set-up was calibrated using low polydispersity poly(methyl methacrylate) standards (PSS, 800–189000 $g \cdot mol^{-1}$).

FT-NIR and -MIR spectra were recorded with a resolution of 2 cm^{-1} on a Fourier transform (FT) spectrometer (Bruker Vertex 70) equipped with an InSb detector, a tungsten lamp and a silicon coated CaF_2 beam splitter. Data acquisition and processing are performed on a personal computer using the OPUS 6.5 software provided by Bruker. A Blackman-Harris three-term function is applied for apodization.

Result and Discussion

Conventional Free Radical Polymerization of VDF and HFP

Reference spectra of the monomers

In the case of the gaseous monomers VDF and HFP, the feed composition was calculated on the basis of the pure component reference spectra, since accurate weighing of these reagents was not possible for the reaction mixture and density data were not available. Thus, even if the absolute monomer quantities in the copolymerization mixture somehow deviate from the desired ones, the actual ratio of the monomers and thus the monomer feed ratio can be determined from the infrared spectra.

The Beer-Lambert law is to be verified, that is:

$$A = \varepsilon \cdot d \cdot c \tag{1}$$

where A is the absorption at a given wavenumber, ε the molar absorptivity, d the optical path length and c the concentration of monomer. It is sometimes convenient to consider the integrated form of this equation, because the integral is less sensitive to temperature and pressure changes:[21]

$$I(\overline{\nu}) = \int \varepsilon(\overline{\nu} \cdot d\,\overline{\nu}) \cdot d \cdot c = B \cdot d \cdot c \tag{2}$$

where I is the area underneath the spectrum and B the integrated molar absorptivity.

The influence of reaction temperature and pressures on the spectra was investigated. A given weighted amount of monomer was first measured at the temperature and the corresponding pressure. Then, CO_2 was added to check for pressure influence. Assuming that the gaseous monomer fills the entire cell volume over all ranges of pressures and temperature, the monomer concentration inside the cell should not change, only eventually the (integrated) molar absorptivities.

In the case of HFP a small path length (0.38 cm) and silicon windows had to be used to observe an absorption peak in the mid-infrared region (around 2100 cm^{-1}) which decreases along with conversion and does not overlap with CO_2 and VDF peaks (see Figure 1). The peak maximum was calculated from a horizontal baseline starting at the minimum of the spectrum between 2140 cm^{-1} and 2110 cm^{-1}. Because this minimum shifted with different pressures and CO_2 contents but not the peak maximum, no integration procedure over

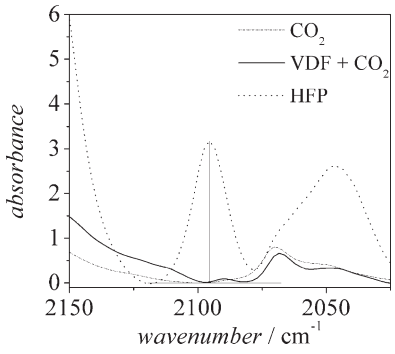

Figure 1.
FT-MIR spectra of the pure components at 100 °C and 800 bar.

the same range of wavenumbers can be applied. Therefore, only the peak maximum is considered. In Figure 1 the peak height and baseline are illustrated.

The concentration dependence of the peak maximum integral, plotted in Figure 2, shows a rather reasonable linear fit, the associated absorptivity is:

$$\varepsilon(\mathrm{HFP},\ 2100\,\mathrm{cm}^{-1},\ 100\,^{\circ}\mathrm{C},\ 800\,\mathrm{bar}) \sim 90\,\mathrm{cm}^2 \cdot \mathrm{mol}^{-1}.$$

Since the HFP concentration is high and 100% HFP conversion cannot be achieved in the experiments (see Figure 6), it is justified to assume a linear behaviour in the high concentration region of the calibration curve.

Although an increase in temperature seemed to enhance the absorptivity, variation of the overall pressure showed a less significant effect on the HFP peaks. It should be noted that due to the use of the same spectroscopic configuration (actually optimized for the NIR region) to observe both peaks simultaneously during the reactions, the resolution of the HFP peak at 2100 cm^{-1} is not as good as the one for VDF at 6303 cm^{-1}.

VDF spectra were recorded with a path length of 1.40 cm, allowing for higher amounts of monomer to be introduced into the cell, reducing the error in weighting. Figure 3 indicates that the characteristic absorption peak of the first overtone of the C–H stretching vibration at the double bond appears at 6303 cm^{-1}. The peak was integrated between 6440 cm^{-1} and 6303 cm^{-1} against a horizontal baseline at 6440 cm^{-1} (shaded area in Figure 3).

The concentration dependence of the VDF integral, plotted in Figure 4, shows a slightly better linear fit than HFP. Although the fit does not go through the origin we believe the estimate is sufficiently close considering the limited accuracy of the weighting method, in particular at low concentrations. The resulting integrated molar absorptivity was determined to be

$$B(\mathrm{VDF},\ 6440 - 6303\,\mathrm{cm}^{-1},\ 100\,^{\circ}\mathrm{C},\ 800\,\mathrm{bar}) \sim 2900\,\mathrm{cm} \cdot \mathrm{mol}^{-1}.$$

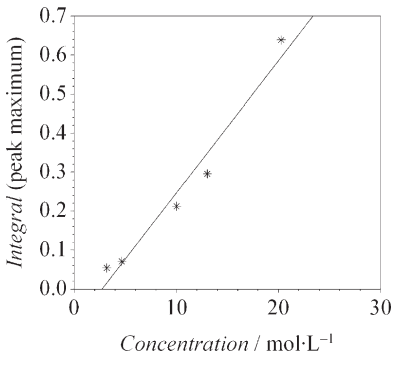

Figure 2.
Variation of the integral of the characteristic HFP peak at 2100 cm^{-1} with HFP concentration at 100 °C, 800 bar, and $d = 0.38$ cm.

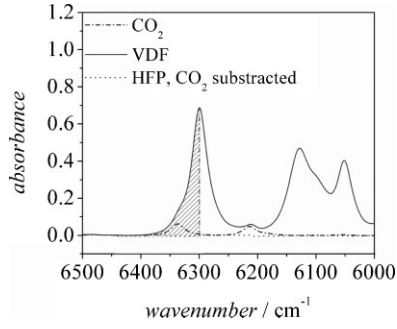

Figure 3.
FT-NIR spectra of pure components at 100 °C and 800 bar.

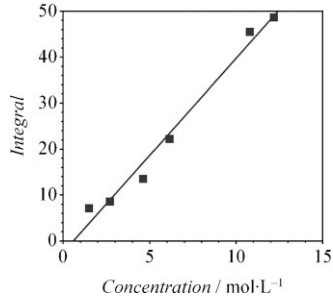

Figure 4.
Variation of the integral of the characteristic VDF peak at 6303 cm^{-1} with VDF concentration at 100 °C, 800 bar, and $d = 1.40$ cm.

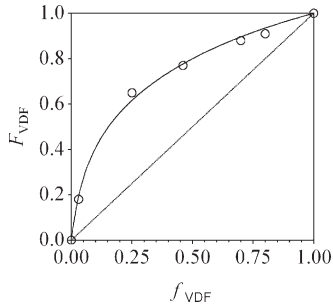

Figure 5.
Copolymer composition diagram from independent experiments up to low conversion. The circles represent the data points and the full line the NLLS fit.

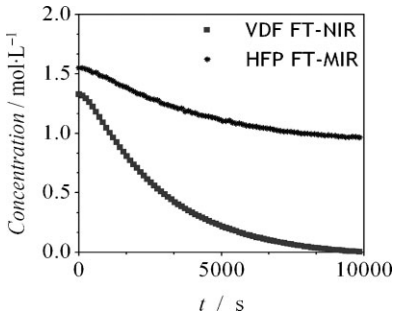

Figure 6.
Concentration vs. time curves of VDF and HFP determined by integration of FT-IR peaks throughout the copolymerization (EM392).

As for HFP, temperature increases the *B* value. However, within experimental error the overall pressure had a minor effect on the VDF spectra.

Table 1.
Experimental conditions for homogeneous phase VDF-HFP copolymerizations with varying VDF content in the monomer feed, f_{VDF}. The VDF content of the copolymer, F_{VDF}, was calculated from FT-NIR- and MIR spectra.

Sample	f_{VDF}	wt.% CO_2	T/°C	p_o/bar	F_{VDF}
EM548[b]	0.03	40	75	900	0.18
EM102[a]	0.25	70	100	800	0.65
EM392[a]	0.46	70	100	900	0.77
EM396[b]	0.70	77	75	910	0.88
EM408[b]	0.80	77	75	1400	0.91

[a][DTBP] = 0.3 mol · L^{-1},
[b][TBPP] = 0.045 mol · L^{-1}.

Copolymerizations of VDF and HFP in homogeneous phase

Five experiments were carried out to full VDF conversion. The experimental details are summarized in Table 1. The reported VDF content in the copolymer, F_{VDF}, was determined from the FT-NIR and -MIR peaks of VDF and HFP, respectively, at about 15% of overall conversion.

Classical approach: calculation of reactivity ratios from several experiments

F_{VDF} and f_{VDF} were determined via in-line spectroscopy, after 15% conversion of VDF. In a first approximation, the reactivity ratios were assumed to be independent of temperature and pressure. The classical Lewis-Mayo equation[22] (eq. 3) was used for a non-linear least square (NLLS) regression analysis of the data points.

$$F_1 = \frac{r_1 f_1^2 + f_1 f_2}{r_1 f_1^2 + 2 f_1 f_2 + r_2 f_2^2} \quad (3)$$

with the reactivity ratios r_1 and r_2. The reactivity ratios obtained are $r_{VDF} = 3.49$ and $r_{HFP} = 0.11$. The values reported in the literature range from $r_{VDF} = 2.45$ to 6.70 and $r_{HFP} = 0$ to 0.12,[10,23–27] encompassing and supporting our results. To improve the accuracy of these reactivity ratios, more data points are needed. However, carrying out multiple laborious high pressure experiments would largely increase the demand of material, time, and energy. As an alternative method for screening a large number

Table 2.
Experimental conditions for full VDF conversion homogeneous phase copolymerizations at 100 °C allowing for broad scanning of monomer feed ratios and the determination of reactivity ratios from single experiments.

Sample	f(VDF)	wt.% CO_2	T/°C	p_0/bar	k_{app}(VDF)/s^{-1}	k_{app} (HFP)/s^{-1}	r_{VDF}	r_{HFP}
EM102	0.25	70	100	800	$2 \cdot 10^{-4}$	$3 \cdot 10^{-5}$	6.85	0.15
EM392	0.46	70	100	900	$4 \cdot 10^{-4}$	$6 \cdot 10^{-5}$	6.79	0.15

of monomer feed ratios over a wide range, in-line spectroscopy is considered.

In-line approach: calculation of reactivity ratios from single experiments

Looking at sets of data point pairs as individual low conversion experiments, one can also directly calculate reactivity ratios from one single experiment, provided that the Beer-Lambert law is valid and that the starting concentrations are well-known.[28] As an example, Figure 6 gives the individual conversions of VDF and HFP for a copolymerization at 100 °C and 900 bar. The data indicate that VDF is preferentially built into the copolymer. At complete VDF conversion around 63% of residual HFP are present.

Because conversions achieved per time interval are rather small, a very scattered set of f_{VDF} vs. F_{VDF} data is obtained, if the raw data is used. In an attempt to determine a 95% joint confidence interval (JCI), the program CONTOUR[29] was used with these raw data. However no convergence could be achieved for most experiments.

Therefore, experimental ln (M_0/M_t) vs. time curves were fitted for each monomer in the linear range (see Figure 7, slopes as k_{app} in Table 2). M_0 is the initial monomer concentration and M_t, the monomer concentration at time t, calculated from the FT-IR conversion data. This procedure gave rise to a copolymer diagram (see Figure 8) with $r_{VDF} \sim 6.80$ and $r_{HFP} \sim 0.15$. A joint confidence interval was not accessible, since fitted raw data were used.

However, small deviations between fit and experimental data may have a large impact on the r values. Figure 9 compares the copolymerization diagram resulting from experimental data chosen at 10% overall conversion intervals and from the entire set of fitted data. In the first case $r_{VDF} = 3.05$ and $r_{HFP} = 0.02$ with a rather poor correlation coefficient were obtained. The second case gives rise to $r_{VDF} = 6.79$ and $r_{HFP} = 0.15$. Thus, this method does not seem as optimum for determining the reactivity ratios of the system.

Combining classical and in-line approach: calculation of reactivity ratios from 10% conversion steps throughout several experiments

Considering larger time intervals than in the previous section was thought to reduce

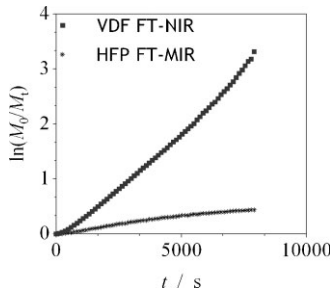

Figure 7.
Individual VDF and HFP conversion vs. time curves for a single in-line experiment (EM392).

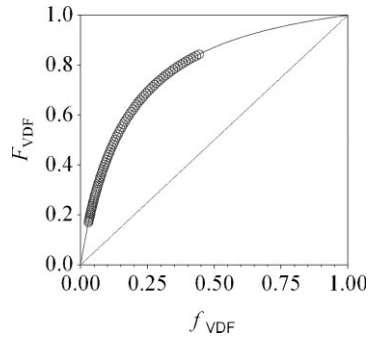

Figure 8.
Copolymerization diagram resulting from the fitted conversion vs. time curves for a single in-line experiment (EM392).

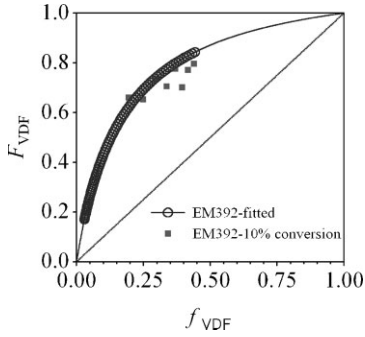

Figure 9.
Comparison of composition data resulting from selected experimental points after 10% conversion steps (full squares) and from all fitted points (open circles).

the scattering between two data points. Intervals corresponding to 10% conversion between 10 and 80% total conversion of VDF were then selected for each experiment. Data points from all individual experiments were included into a single data set (4 experiments with 8 points each) for the derivation of reactivity ratios. The corresponding copolymerization diagram is shown in Figure 10, together with the 95% joint confidence interval resulting from the CONTOUR algorithm. Finally, the estimated values of the reactivity ratios are $r_{VDF} = 4.34$ and $r_{HFP} = 0.11$, which are in the upper range of the literature data reported. The 95% JCI is represented by a slightly asymmetrical ellipse, reflecting the non-linearity of the system. In future work, the systems should be analyzed with an updated version of CONTOUR that will take into account errors in both monomer conversion and monomer feed ratio.

However, it can already be concluded that this method allows for the derivation of *r* values on the basis of a rather small set of experiments that produces an extended set of data. The pressure and temperature influence on the reactivity ratios can thus be investigated in more detail thanks to this in-line approach.

AGET ATRP of F-Decene and tBA

Spectroscopic Analyses

NIR spectra of F-decene and *t*BA depicted in Figure 11 show characteristic absorption peaks assigned to the C–H-stretching vibration of the unsaturated C-atom at 6197 cm^{-1} for F-decene and at 6163 cm^{-1} for *t*BA. The spectrum of pure CO_2 is shown for comparison. The optical path lengths for the monomer spectra and for CO_2 are 2 and 9.9 mm, respectively.

A typical FT-NIR spectra series of an F-decene - *t*BA copolymerization at 115 °C and p_0 of 1000 bar is given on the left hand side in Figure 12. The spectra series shows the decrease of the overlapping monomer peak. It is evident that the decrease in intensity is more pronounced for *t*BA, indicating that *t*BA is preferentially incor-

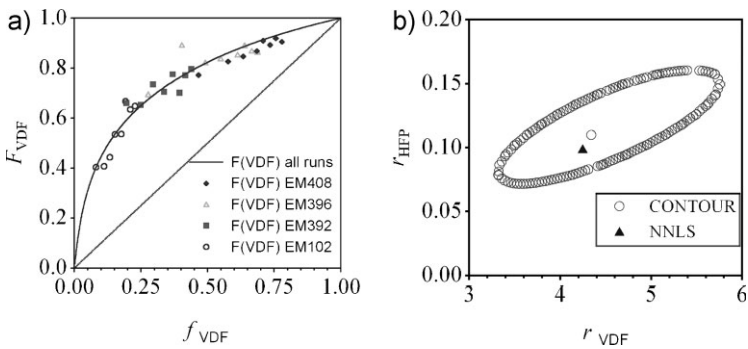

Figure 10.
(a): Copolymer composition diagram resulting from several in-line experiments, selecting data points every 10% conversion steps. (b): Reactivity ratios and 95% JCI from several in-line experiments, selecting data points every 10% conversion steps.

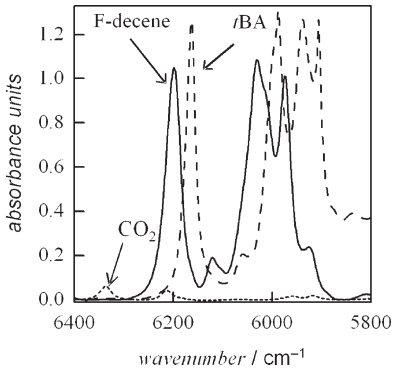

Figure 11.
NIR spectra of CO_2 ($d = 9.9$ mm, $T = 115\,^{\circ}C$, $p = 900$ bar), F-decene and *t*BA ($d = 2$ mm, $T = 25\,^{\circ}C$, $p = 1$ bar).

Livingness of the system

F-decene-*t*BA copolymerizations in solution with $scCO_2$ were carried out in homogeneous phase. To achieve good solubility of the catalyst and to ensure good control of the polymerization a Cu catalyst with the fluorinated ligand F-TEDETA (see Scheme 1) was used. Table 3 gives the results of five AGET ATRP copolymerizations of F-decene and *t*BA at 115 °C and an initial pressure of 1000 bar with varying mole fractions of F-decene in the monomer feed, $f_{\text{F-decene}}$, and *t*BA, $f_{t\text{BA}}$, at a constant CO_2 content of 40 wt.%. All reactions were carried out with the following concentration ratios:

$$[\text{monomer}] : [\text{EBIB}],\ 1 : 0.02$$
$$[\text{EBIB}] : [\text{CuBr}_2] : [\text{F} - \text{TEDETA}] : [\text{Sn(EH)}_2],\ 5000 : 100 : 1 : 15.$$

porated into the polymer. The individual conversions of each monomer cannot directly be calculated from the overlapping peak. However, deconvolution of the original spectrum via the OPUS software yields two single peaks (see Figure 12b), that allow for calculation of individual monomer conversions. To test for the quality of spectra obtained from deconvolution, the superposition of the two monomer peaks is contained in Figure 12b, too. The agreement with the original spectra between 6140 and 6260 cm^{-1} is excellent.

Figure 13 shows molecular weight distributions from copolymers where the mole fraction of F-decene in the monomer feed was 0.5. The number average molar masses range from 8000 to 18200 $g \cdot mol^{-1}$ and the polydispersities from 1.3 to 2.6. To test for livingness of the polymerizations the evolution of molecular weight with monomer conversion was checked. The molecular weight distributions depicted in Figure 13 show a modest shift to higher molecular weights with increasing conversion, which suggests that controlled polymerizations

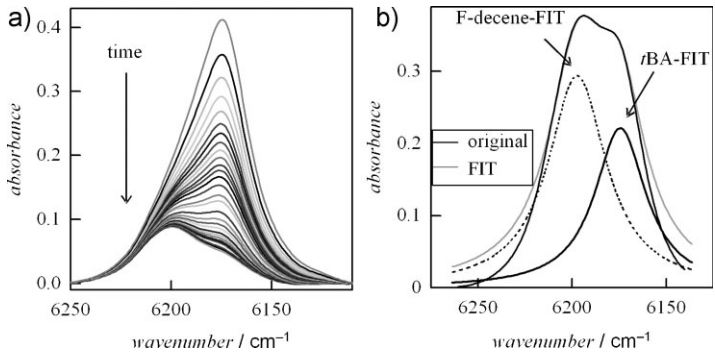

Figure 12.
Absorption spectra of F-decene – *t*BA copolymerization. a) Original spectra series, b) *t*BA and F-decene spectra after deconvolution, superposition of the *t*BA and F-decene spectra and original spectrum. For further details the reader is referred to the text.

Table 3.
Results of F-decene - *t*BA copolymerizations in $scCO_2$[a]

sample	$f_{F\text{-decene}}$	*t*/h	*overall conversion*[b]	M_n/g·mol^{-1}	*PDI*	$F_{F\text{-decene}}$[b]	$F_{F\text{-decene}}$[c]
US 93	0.8	2.5	12	8000	2.1	0.18	0.25
US 94	0.7	3.6	20	11300	1.7	0.14	n.a.
US 103	0.5	1.5	24	12200	1.3	0.06	n.a.
US 92	0.4	1.9	27	10000	2.0	0.06	n.a.
US 95	0.1	0.5	26	18 200	2.6	0.03	0.07

[a]Reaction conditions: [monomer]: [EBIB], 1: 0.02; [EBIB]: [$CuBr_2$]: [F-TEDETA]: [$Sn(EH)_2$], 5000: 100: 1: 15: 15; 40 wt. % CO_2, $T = 115\,^{\circ}C$, initial pressure of 1000 bar. $f_{F\text{-decene}}$: mole fraction of 1H, 1H, 2H perfluoro-1-decene in the monomer feed, M_n: number average molecular weight, *PDI*: polydispersity, $F_{F\text{-decene}}$: mole fraction of 1H, 1H, 2H perfluoro-1-decene in the polymer, n.a.: not available.
[b]from IR data.
[c]from ^{19}F-NMR.

were carried out. This conclusion is supported by comparison with SEC-results from a free radical polymerization using *tert*-butyl peroxy-2-ethylhexanoate as initiator: the conventional radical polymerizations yields polymer material with molecular weights around 10^5 g·mol^{-1} and high polydispersity. Currently, the catalyst system is optimized to yield narrower molecular weight distributions. In addition, chain extension experiments will be carried out to check, if a living system was established.

Reactivity Ratios

As detailed above, the conversion – time data of each monomer may be used to calculate the reactivity ratios of the copolymerization. In 19 independent experiments the data referring to the initial 10% overall conversion were considered. After deconvolution of the monomer absorption peak, individual conversions of F-decene and *t*BA were accessible. The data were used to calculate corresponding $f_{F\text{-decene}}$ and $F_{F\text{-decene}}$ values, which are plotted in the copolymerization diagram in Figure 14. According to the Lewis-Mayo equation (eq. (3)), the reactivity ratios may be obtained from a non-linear least-squares regression analysis. The line in Figure 14 represents the variation of $F_{F\text{-decene}}$ with $f_{F\text{-decene}}$ as determined from the NLLS analysis. The reactivity ratios are

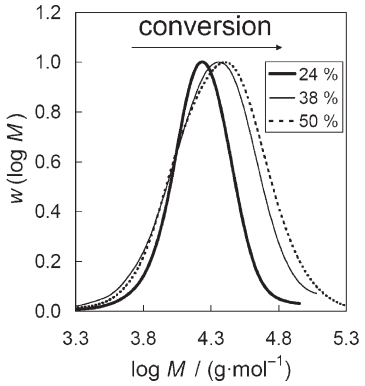

Figure 13.
Molecular weight distribution of copolymers from reactions with $f_{F\text{-decene}} = 0.5$.

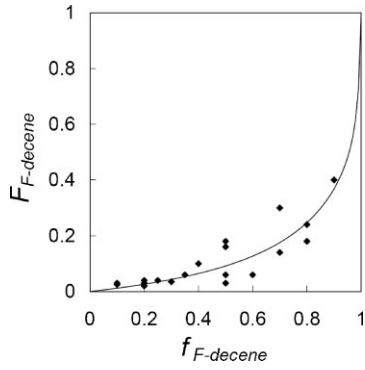

Figure 14.
Mole fractions of F-decene in the monomer feed, $f_{F\text{-decene}}$, and in the polymer, $F_{F\text{-decene}}$, with Lewis Mayo non linear least square regression of several independent experiments. Reaction conditions: [monomer]: [EBIB], 1: 0.02; [EBIB]: [$CuBr_2$]: [F-TEDETA]: [$Sn(EH)_2$], 5000: 100: 1: 15: 15, 40 wt. % CO_2; $T = 115\,^{\circ}C$; $p_0 = 1000$ bar.

$r_{t\mathrm{BA}} = 9.12$ and $r_{\text{F-Decene}} = 0.019$. The 95% confidence interval calculated with the Contour program indicates a high uncertainty, because of the very low reactivity ratio for F-decene. Since literature data for the system under consideration are not available, data reported for a non-fluorinated system are considered. The reactivity ratios for methyl acrylate (MA) – 1-octene copolymerizations[30] were determined to be $r_{\mathrm{MA}} = 7.5$ and $r_{\text{1-octene}} = 0$ and *t*BA – 1-octene copolymerizations are assoziated with and $r_{t\mathrm{BA}} = 31.9$ and $r_{\text{1-Octene}} = 0.007$. The data indicate that in all cases the acrylate is preferentially built into the polymer. The findings may be explained by the poor stabilisation of the primary radical with a terminal F-decene or 1-octene unit, in contrast to the rather good stabilizations of the secondary radical with a terminal acrylate unit. Although the uncertainty of the reactivity ratios is rather high, the data suggest that the fluorinated C-atoms in the neighbourhood of the reactive double bond and thus the radical functionality lead to a better stabilization of the radical than in case of the non-fluorinated alkene.

Conclusions

Conventional VDF-HFP copolymerizations and AGET ATRP copolymerizations of F-decene and *t*BA were carried out in homogeneous phase of $scCO_2$ up to complete monomer conversion. FT-NIR spectroscopic in-line monitoring of the reactions and deconvolution of the spectra give access to the conversions as a function of time for each monomer individually. Deriving a number of monomer feed - copolymer composition data pairs for each experiment, only a small number of high-pressure experiments is sufficient to determine the reactivity ratios. Joint confidence intervals of the reactivity ratios calculated for both copolymerization systems indicate that the reactivity ratios for VDF and *t*BA, which are preferentially built into the VDF – HFP and *t*BA - F-decene copolymer, respectively, are accessible with good precision. Due to the very low incorporation of HFP and F-decene in the copolymers, the associated reactivity ratios are less precise. Currently, modelling of VDF – HFP systems is in progress to obtain a more detailed understanding of the copolymerization mechanisms.[9,31,32]

Acknowledgements: The authors are grateful to *Deutsche Forschungsgemeinschaft* (DFG, BE2032/2-1) and to *Dyneon GmbH* for financial support.

[1] S. Beuermann, M. Buback, C. Isemer, A. Wahl, *Macromol. Rapid Commun.* **1999**, *20*, 26.
[2] L. Du, J. Y. Kelly, G. W. Roberts, J. M. DeSimone, *J. Supercrit. Fluids* **2009**, *47*, 447.
[3] F. Rindfleisch, T. P. DiNoia, M. A. McHugh, *J. Phys. Chem.* **1996**, *100*, 15581.
[4] J. P. Giesy, K. Kannan, *Environ. Sci. Technol.* **2001**, *35*, 1339.
[5] J. M. DeSimone, Z. Guan, C. S. Elsbernd, *Science* **1992**, *257*, 945.
[6] S. Beuermann, M. Imran-ul-haq, *J. Polym. Sci., Part A: Polym. Chem.* **2007**, *47*, 5626.
[7] M. K. Saraf, S. Gerard, L. M. Wojcinski, P. A. Charpentier, J. M. DeSimone, G. W. Roberts, *Macromolecules* **2002**, *35*, 7976.
[8] A. Galia, G. Caputo, G. Spadaro, G. Filardo, *Ind. Eng. Chem. Res.* **2002**, *41*, 5934.
[9] P. A. Mueller, G. Storti, M. Morbidelli, M. Apostolo, R. Martin, *Macromolecules* **2005**, *38*, 7150.
[10] U. Beginn, R. Najjar, J. Ellmann, R. Vinokur, R. Martin, M. Moeller, *J. Polym. Sci., Part A: Polym. Chem.* **2006**, *44*, 1299.
[11] S. Ebnesajjad, *Fluoroplastics.*, Volume 2: *melt processable fluoropolymers, the definitive user's guide and databook*, Plastic Design Library, Norwich, NY **2003**.
[12] A. L. Moore, *Fluoroelastomer Handbook, the definitive user's guide and databook*, Plastic Design Library, Norwich, NY **2006**.
[13] S. Borkar, A. Sen, *Macromolecules* **2005**, *38*, 3029.
[14] G. Davis, M. G. Broadhurst, A. J. Lovinger, T. Furukawa, *Ferroelectrics* **1984**, *57*, 73.
[15] M. Wegener, W. Künstler, K. Richter, R. G. Multhaupt, *J. Appl. Phys.* **2002**, *92*, 7442.
[16] K. Min, H. Gao, K. Matyjaszewski, *J. Am. Chem. Soc.* **2005**, *127*, 3825.
[17] P. Kwiatkowski, J. Jurczak, J. Pietrasik, W. Jakubowski, L. Mueller, K. Matyjaszewski, *Macromolecules* **2008**, *41*, 1067.
[18] T. Arita, M. Buback, O. Janssen, P. Vana, *Macromol. Rapid Commun.* **2004**, *25*, 1376.

[19] B. Grignard, C. Jérôme, C. Calberg, R. Jérôme, C. Detrembleur, *Eur. Polym. J.* **2008**, *44*, 861.
[20] M. Buback, H. Latz, *Macromol. Chem. Phys.* **2003**, *204*, 638.
[21] M. Buback, *Angew. Chem. Int. Ed. Engl.* **1991**, *30*, 641.
[22] F. R. Mayo, F. M. Lewis, *J. Am. Chem. Soc.* **1944**, *66*, 1594.
[23] G. Moggi, P. Bonardelli, S. Russo, *6th Conv. Ital. Sci. Macromol., [Atti]* **1983**, *2*, 405.
[24] M.-P. Gelin, B. Ameduri, *J. Fluorine Chem.* **2005**, *126*, 577.
[25] H. Tai, W. Wang, S. M. Howdle, *Macromolecules* **2005**, *38*, 9142.
[26] T. S. Ahmed, J. M. DeSimone, G. W. Roberts, *Macromolecules* **2006**, *39*, 15.
[27] T. S. Ahmed, J. M. DeSimone, G. W. Roberts, *Macromolecules* **2008**, *41*, 3086.
[28] S. Shaikh, J. E. Puskas, G. Kaszas, *J. Polym. Sci., Part A: Polym. Chem.* **2004**, *42*, 4084.
[29] A. M. van Herk, *J. Chem. Educ.* **1995**, *72*, 138.
[30] R. Venkatesh, S. Harrisson, D. M. Haddleton, B. Klumperman, *Macromolecules* **2004**, *37*, 4406.
[31] M. Apostolo, V. Arcella, G. Storti, M. Morbidelli, *Macromolecules* **1999**, *32*, 989.
[32] I. A. Quintero-Ortega, E. Vivaldo-Lima, R. B. Gupta, G. Luna-Bárcenas, A. Penlidis, *J. Polym. Sci., Part A: Polym. Chem.* **2007**, *44*, 205.

